Desalination and Water Treatment
www.deswater.com
1944-3994/1944-3986 © 2013 Desalination Publications. All rights reserved
doi: 10.1080/19443994.2012.693698

51 (2013) 988–996
January

Taylor & Francis
Taylor & Francis Group

Antibacterial efficiency of composite nano-ZnO in biofilm development in flow-through systems

Avner Ronen[a], Rafael Semiat[b], Carlos G. Dosoretz[a,*]

[a]*Civil and Environmental Engineering, and Grand Water Research Institute, Technion-Israel Institute of Technology, Haifa 32000, Israel*
Tel. +972 4 8294962; Fax: +972 4 8228898; email: carlosd@tx.technion.ac.il
[b]*Chemical Engineering, and Grand Water Research Institute, Technion-Israel Institute of Technology, Haifa 32000, Israel*

Received 12 March 2012; Accepted 10 May 2012

ABSTRACT

Biofouling and its control is an acute problem in all water-flowing systems. Inorganic nanoparticles (np) such as zinc oxide (ZnO) exhibit strong antibacterial activities on a broad spectrum of bacteria even when mixed within polymers. Most research until now tested the antibacterial ability only in static conditions. The current research studied the ability of ZnO np to suppress bacterial attachment and biofilm development under flowing conditions, either embedded in polymethyl methacrylate (PMMA) or entrapped in polyacrylamide gel. The composite ZnO np films were characterized by high resolution- scanning electron microscopy and energy-dispersive X-ray spectroscopy, and their antibacterial abilities were evaluated using inhibition zone in agar plates and direct contact in liquid media. In all cases studied, bacterial adhesion was significantly prevented, while the control sample showed biofilm development. Interestingly, a lower antibacterial activity was found in all cases under flowing conditions as compared to static conditions. In batch conditions, it was found that the antibacterial mechanism is based on reactive oxygen species release from the ZnO np. A composite ZnO–PMMA film was designed to mimic a feed spacer with antibacterial abilities in a membrane separation process, and the biofilm development was evaluated. The composite feed spacer displayed promising ability in delaying biofilm development in membrane filtration trials.

Keywords: Biofouling; Zinc oxide; Nanoparticles; Membrane separation; ROS

1. Introduction

Biofouling is the most complex and difficult-to-solve form of fouling and appears in all water-related flow systems. Biofouling is defined operationally and refers to the amount of biofilm development that interferes with technical or economic requirements. A biofilm is a microbial aggregate that occurs at the interface of any flowing system. Microorganisms are present in nearly all water treatment systems, and they tend to adhere to surfaces and grow, mainly by using nutrients extracted from the water phase. A feature

*Corresponding author.

Presented at the International Conference on Desalination for the Environment, Clean Water and Energy, European Desalination Society, 23–26 April 2012, Barcelona, Spain

that all biofilms have in common is that the organisms are embedded in a matrix of microbial origin, consisting of extracellular polymeric substances (EPS). Once biofilms form, they can be very difficult to remove. The EPS impart the characteristic properties of biofilms, and among them is the remarkable resistance to biocides that would otherwise kill them in the planktonic state [1,2]. Disinfection of the feed water using chlorine is the most common treatment for biofouling prevention but may have severe influence on membrane's systems by damaging the membrane active layer. In other flow systems, use of chlorine may cause the formation of harmful disinfection byproducts, which have been proven as carcinogens [3,4].

Generation of antibacterial surfaces using antimicrobial nanomaterials is the envisioned technology to suppress biofilm growth. Methods to generate antibacterial surfaces include addition of antibacterial chemicals or synthesizing super-hydrophobic surfaces [5,6].

Inorganic materials, and especially metal oxides, have attracted lots of attention over the past decade due to their ability to withstand harsh process conditions. They have been known to have strong inhibitory and bactericidal effects as well as a broad spectrum of antimicrobial activities. Nanoparticles (np) made from metal oxides with sizes <100 nm exhibit antimicrobial activities owing to their special characteristics, for example small particle size and large surface area [7].

Zinc oxide (ZnO) nanoparticles exhibit strong antibacterial activities on a broad spectrum of bacteria, including selective toxicity for prokaryotic and eukaryotic systems [8,9]. However, the mechanism of the antibacterial activity of ZnO is not fully understood. Studies have proposed several mechanisms of antibacterial activity of ZnO np. The photocatalytic generation of hydrogen peroxide (H_2O_2) was suggested to be one of the primary mechanisms, and a linear correlation was found between the concentration of ZnO particles and the concentration of H_2O_2 produced [10]. ZnO np is known to be photo-catalytic under UV light although recent research has shown antibacterial activity at dark conditions too [11].

In addition, penetration of the cell envelope and disorganization of bacterial membrane, and interaction of intracellular contents with np upon contact with ZnO np were indicated to inhibit bacterial growth [8,12]. It was found that nanometer-scale ZnO is considerably more efficient in killing bacteria than micrometer-scale particles [8]. Furthermore, a clear correlation between the decreased particle size and increased amount of hydroxyl radicals was found. It has also been postulated that the inhibitory efficacy of ZnO np is concentration dependent [12].

Several research studies showed the ability of ZnO np to attach to and embed in a polymer matrix. The composite film has shown antibacterial properties similar to the ZnO np [12–14].

Almost all research done on the antibacterial activity of ZnO np (with or without polymers) was carried out in static conditions without taking into account the influence of flow on the enhanced biofilm formation under flow conditions [15–17]. Biofilm growth is influenced by many factors [18], including decrease in nutrients and protection from harmful conditions. When tested in static conditions, bacteria were not exposed to any disturbance and discomfort, which encourages biofilm growth. In flow conditions, a bacterium that is not connected to the biofilm is removed from the system. Exposure to diluted concentration of medium also encourages biofilm growth [19].

The present research examined the antibacterial ability of ZnO np embedded in polymers under flow conditions. Understanding the differences in antibacterial activity of ZnO np between static and flow conditions will be helpful in creating efficient antibacterial surfaces able to work in "real-life" conditions. A simple embedding by polymer casting was applied for mimic a polymeric spacer which is a part of membrane separation modules operating in spiral wound configuration. The antibacterial activity of the spacer was examined in a flow-through system with model bacteria.

2. Materials and methods

All materials were used without further purification. ZnO np (<100 nm diameter), zinc acetate hexahydrate, polymethyl methacrylate (PMMA), methyl acrylate, polyethylene glycol 400 (PEG 400), acrylamide, and glutaraldehyde were all of chemical pure grade (Sigma-Aldrich).

Pseudomonas putida strain S-12 (ATCC 700801) was used as the model organism in this study [19]. Luria–Bertani (LB) medium was purchased from Sigma-Aldrich and used for growing bacterial cultures and in flow experiments. Flat-sheet polysulfone membranes of 200 KDa molecular weight cut-off (mwco) were obtained from GE Osmonics (ymersp3001).

2.1. Preparation of ZnO coating/ZnO embedding in polymer

ZnO np were applied to the polymers by solution casting in which the np are embedded or by gel synthesis in which the np are entrapped within the polymer.

PMMA–ZnO np composite film (embedded)—PMMA (2% w/w) and ZnO np (50% w/w of PMMA)

were mechanically mixed as dry powder, then acetone (20 mL) and polyethyleneglycol (PEG 400, 10% w/w of ZnO) were added, and the suspension was sonicated for 60 min in a sonication bath. Afterward the solution was magnetically stirred overnight before casting. Samples were then dried at room temperature overnight.

PAA–ZnO np gel (entrapped)—polyacrylamide (PAA) gel was prepared following a standard procedure [20]. The gel contained 3% (w/w) ZnO np.

2.2. Morphological observations

High-resolution scanning electron microscopy (HRSEM) was performed using a Zeiss Ultra plus high-resolution scanning electron microscope at a voltage of 1 KV. Prior to imaging samples, were fixed using 3% glutaraldehyde and dehydrated using an ethanol gradient under cold conditions, as described elsewhere [21]. Finally, samples were left overnight in 100% ethanol. Energy-dispersive X-ray spectroscopy was performed after coating with a thin carbon layer using an FEI E-SEM Quanta 200. Before imaging, samples were washed with double distilled water (DDW) and dried at room temperature overnight.

2.3. Antibacterial activity

The inhibition clearing zone assay on agar plates was used to determine the inhibition zone of ZnO-coated films against *P. putida* S-12. Samples of composite polymers were cut into disks and then placed on LB plate previously inoculated with 100 μL of inoculum containing approximately 10^8–10^7 CFU mL^{-1} of tested microorganisms. The plates were incubated at 37˚C for 48 h, and then the diameters of the inhibition zone of the films were determined.

The antimicrobial activity of the composite film was also tested in static liquid cultures. One milliliter of saline containing 10^8–10^6 CFU mL^{-1} of *P. putida* S-12 was seeded on the composite film for specific time durations. Following the contact, samples of the liquid were plated on LB medium for living cell counts.

Bacterial colonization in flow through systems tests was compared with that in a control flow cell containing an unmodified sample. During the experiment the volumetric flow was set-up similar in both cells. Moreover, after the run ended, samples were washed in saline and underwent further visualization and analysis by HRSEM.

ROS release from the composite ZnO np film was tested using *p*-benzoic acid (PABA), which acted as a scavenger of ROS [22]. Initial PABA concentration was 400 ppb (measured by HPLC-MS). A 2×3 cm^2 composite ZnO np film was added to the PABA solution and compared with 0.1% w/w ZnO np solution with the same concentration of PABA. Both samples were magnetically stirred during the

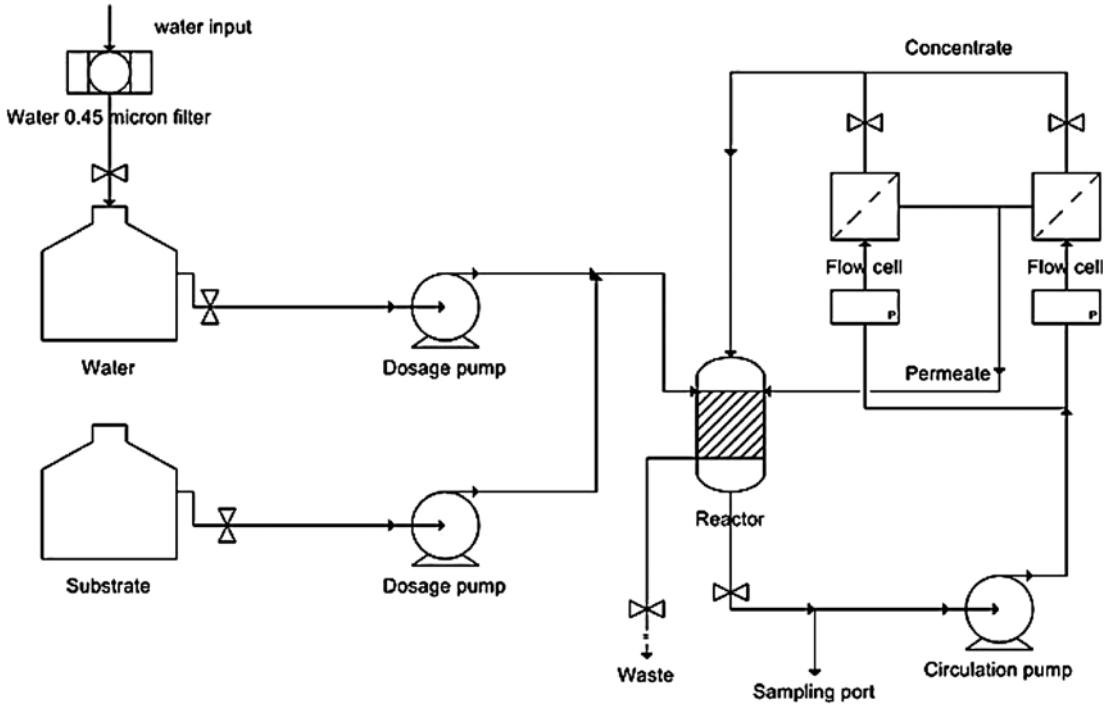

Fig. 1. Schematic design of the experimental flow-cell system.

experiment. Samples were extracted from both solutions and tested for the PABA concentration changes with respect to time.

2.4. Flow-through experiments

Flow-through experiments were conducted using a modular a two-channel planar flow-cell system similar to that described elsewhere [19]. A nutrient stream consisting of LB medium diluted in place 100-fold with filtered tap water (0.2 μm filter, Pall) was fed into a 140 ml reactor by means of two parallel peristaltic pumps (Cole-Parmer). The final dilution in the reactor is 100 times than LB medium. The different components of the system were connected with silicone tubing, and recirculation was accomplished using a peristaltic pump. Biofilms of *P. putida* were allowed to develop under sterile conditions. All components of the system, with the exception of the flow cells (made of polycarbonate) and pressure gauges, underwent sterilization by autoclaving (121 ℃ for 20 min) before each experiment. After assembling of the system, 0.5% NaOCl solution was flushed for 24 h, and then was thoroughly rinsed with filtered tap water for several hours and finally with experimental medium. Then, the system was inoculated to the indicated bacterial concentration. The retention time in the whole system was set to 15 min to ensure washout of suspended bacteria. The volumetric flow rate in the cells was fixed at typical laminar regime (Reynolds number was 200–600) by means of the recirculation pump. A schematic view of the entire system is shown in Fig. 1.

3. Results and discussion

3.1. Antibacterial activity of composite PMMA–ZnO np

First, the results concerning the PMMA–ZnO composite are presented. The PMMA–ZnO np composite film was casted and dried overnight at room temperature. Its morphological characterization was analyzed by HRSEM (Fig. 2). Samples were cut from the flexible composite film and imaged. Images were compared to control samples made from cast PMMA without ZnO np.

The ZnO np embedded in the PMMA film could be clearly observed on the surface layer (Fig. 2(C) and (D)) compared to the morphology of the control PMMA film (Fig. 2(A) and (B)). As can be seen, the ZnO np was dispersed almost uniformly in the entire polymer matrix covering the whole surface, although a few particles of agglomerates were evident. Similar results were reported mixing polypropylene with ZnO micro particles as powder and then mold-injecting them [23]. When using ZnO np, a better coverage of

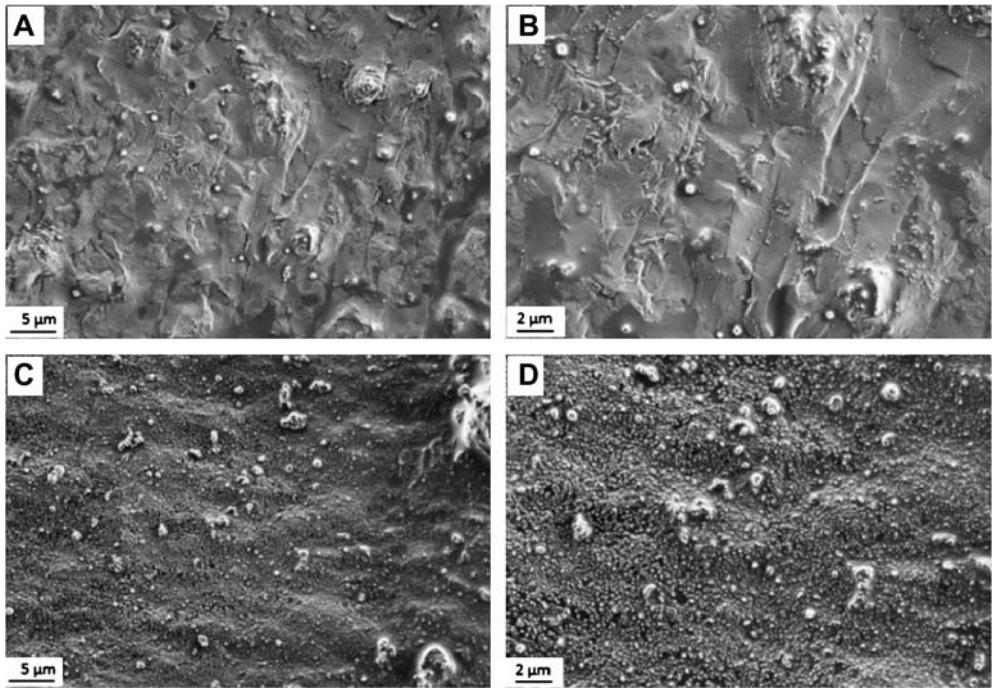

Fig. 2. HRSEM micrographs of virgin composite PMMA–ZnO and PMMA films casted. Upper panels: PMMA control (A ×5 K; B ×10 K magnification). Bottom panels: PMMA–ZnO (C ×5 K; D ×10 K magnification).

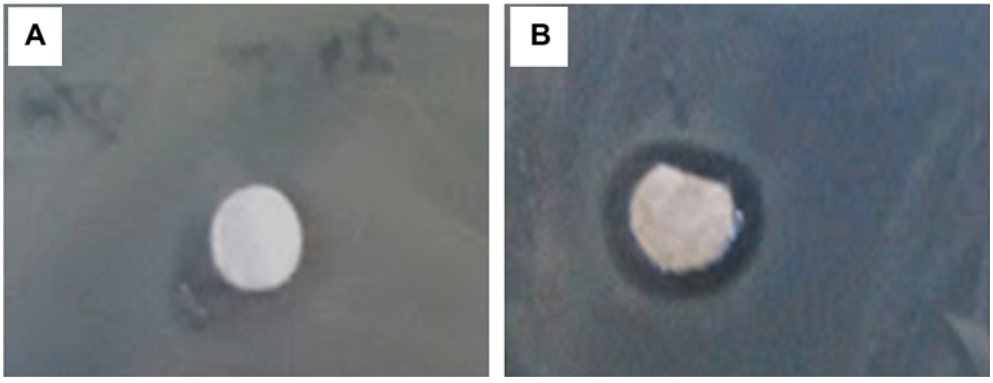

Fig. 3. Inhibition clearing zone test for composite PMMA–ZnO films on LB agar medium. (A) PMMA without ZnO np (control). (B) PMMA–ZnO np composite. Plates were inoculated with *P. putida* S-12 and were incubated for 48 h.

the surface was observed due to the increased amount of particles at the same weight loading [24].

The antibacterial abilities in static conditions were tested by the inhibition zone method on LB agar plates (Fig. 3). A inhibition clearing zone with a radius of about 5 mm could be seen around the sample, proving the antibacterial influence compared to the control PMMA film without ZnO np.

Direct contact of saline containing 10^8 CFU mL^{-1} of *P. putida* S-12 with the composite ZnO np film was tested in static liquid cultures for 6 and 18 h. Following the contact, samples of the liquid were plated on LB medium for living cell counts. The composite film exhibited 4 logs reduction (killing rate of 99.99%) after 6 h of contact and 6 logs reduction after 18 h (killing rate of 99.99%). As the np were embedded in a polymer matrix and were unable to diffuse, ROS release might probably be the most influencing antibacterial factor. The release of ROS was reported as part of the antibacterial mechanisms for metal oxides in general and ZnO in particular, among other mechanisms involving direct contact [8,10]. Our results fit literature reports, showing the antibacterial ability of ZnO np embedded in polypropylene film by direct contact [23]. The composite polypropylene film eliminated more than 99.90% of the model bacteria *Staphylococcus aureus* and *Klebsiella pneumonia* after 24 h.

ROS release from the composite ZnO np film was compared to a ZnO np suspension using *p*-benzoic acid (PABA) in saline as a scavenger (Fig. 4). Initial ZnO concentrations (w/w) were similar in both samples (1 mg mL^{-1}). The decrease rate in ZnO np was found to be almost similar in both tested samples derived from the presence of ZnO np. The decrease in PABA concentration with time followed an exponential trend indicating a first-order reaction in both cases, as typical for the involvement of ROS release. Initial ZnO np concentrations (w/w) were almost similar in both samples. The free ZnO np displayed a slightly increased reduction in PABA concentration compared to the embedded np, probably due to the high surface area of exposure.

Zinc ion diffusion from the film could influence the antibacterial clearing as well [25]. Therefore, leaching of zinc ions from the film was tested in two controlled water backgrounds (DDW and synthetic sea water) for a period of two weeks. Samples were immersed in the solution and shaken (150 rpm) during the course of the experiment. After 7 and 14 days, 5 mL of the sample solution was filtered (0.25 μm) and tested for zinc ions by inductively coupled plasma. Results indicated negligible traces of zinc ions in both samples. Similar results were reported in the literature, indicating that the antibacterial ability was not a result of released ions [25].

The ability of the composite PMMA–ZnO np to suppress biofilm formation was further tested in a flow-through cell system at laminar flow regime (Re ≈ 200–600), employing *P. putida* S-12 as model bac-

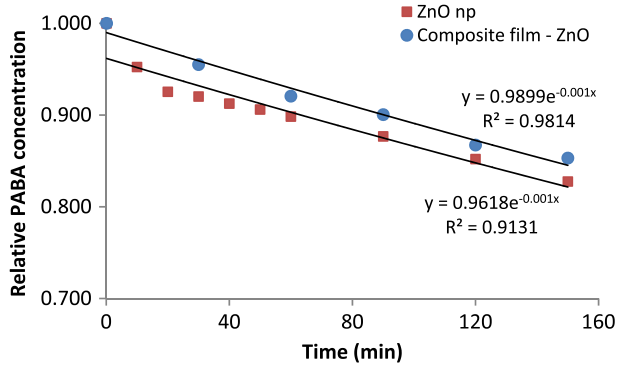

Fig. 4. PABA decay (relative concentration) in the presence of ZnO np. Initial ZnO np concentrations were 1 mg mL^{-1} in both samples.

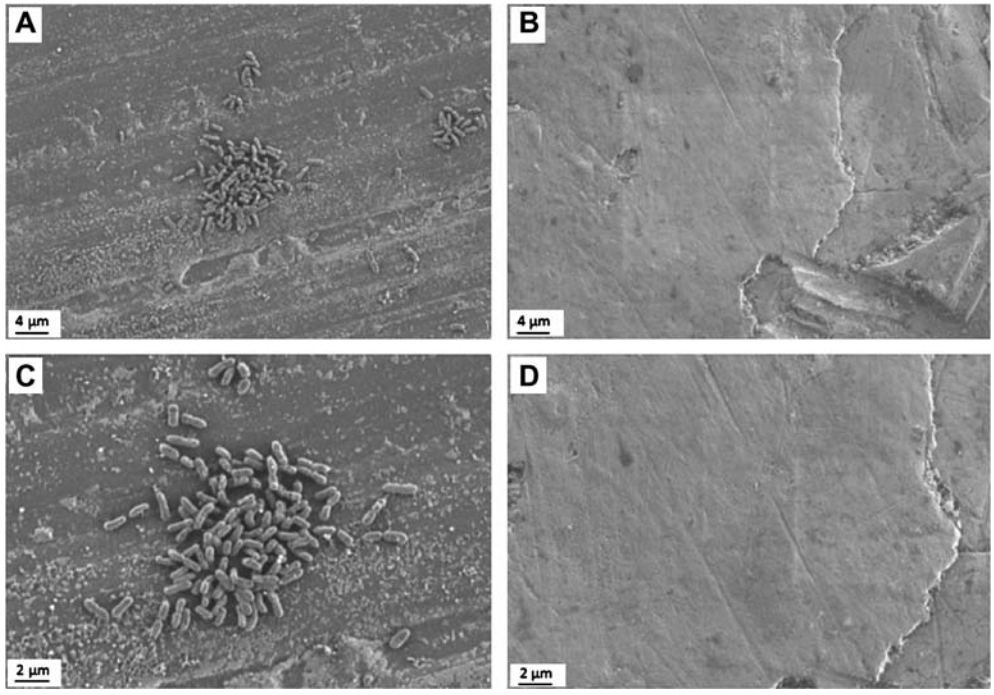

Fig. 5. HRSEM micrographs of composite PMMA–ZnO and PMMA films at the end of the flow-through run in the presence of a *P. putida* S-12 suspension (10^3 CFU mL^{-1} for 48 h at Re ~ 600). Left panel: control—PMMA film (control) (A ×5 K; C ×10 K magnification). Right panel: composite PMMA–ZnO-PEG 400 film (B ×5 K; D ×10 K magnification).

terium. A preliminary set of experiments with composite ZnO np casted in the absence of PEG was performed using a high initial bacteria concentration of 10^8 CFU mL^{-1} (data not shown). Both control and composite films exhibited bacterial deposition; however, a developed biofilm layer was observable on the surface of the control, whereas sporadic-dispersed attached bacteria in monolayer were found on the PMMA–ZnO composite. In order to improve the dispersion of the ZnO np, PEG 400 was used at the amount of 10% from the amount of ZnO np. PEG was reported to stabilize ZnO np in casted PVC films and help to prevent coagulation [26].

A second set of experiments was performed with a low bacteria concentration (10^3 CFU mL^{-1}) and the same hydraulic parameters. Flow-through experiments with the PMMA–ZnO composite film showed improved results (Fig. 5). HRSEM images of the control PMMA film showed several areas with attached bacteria (Fig. 5(A) and (C)), while images of composite PMMA–ZnO film (Fig. 5(B) and (D)) showed no adhered bacteria. We could not find in the literature any data regarding ZnO composite surfaces in flow conditions. It should be noted that only although a limited amount of the ZnO np are on the surface of the composite material while embedding the np in the polymer matrix, a very high antibacterial efficiency was attained.

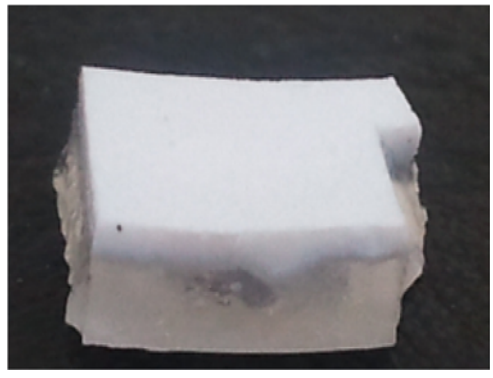

Fig. 6. Close-up view of the PAA–ZnO np gel with np entrapped on its surface.

3.2. Antibacterial activity of PAA–ZnO np gel

In order to further verify the antibacterial efficiency of the ZnO np under flow conditions, a PAA gel with ZnO np (3% w/w) entrapped on the very top surface of the gel was synthesized (Fig. 6). At difference from the PMMA casted composite, the composite gel is water permeable.

First, the antimicrobial activity of the PAA–ZnO gel was tested in static liquid cultures for 1 and 2 h of incubation with 10^6 CFU mL^{-1} of *P. putida* S-12. Following the contact, samples of the liquid were plated on LB medium for living cell counting.

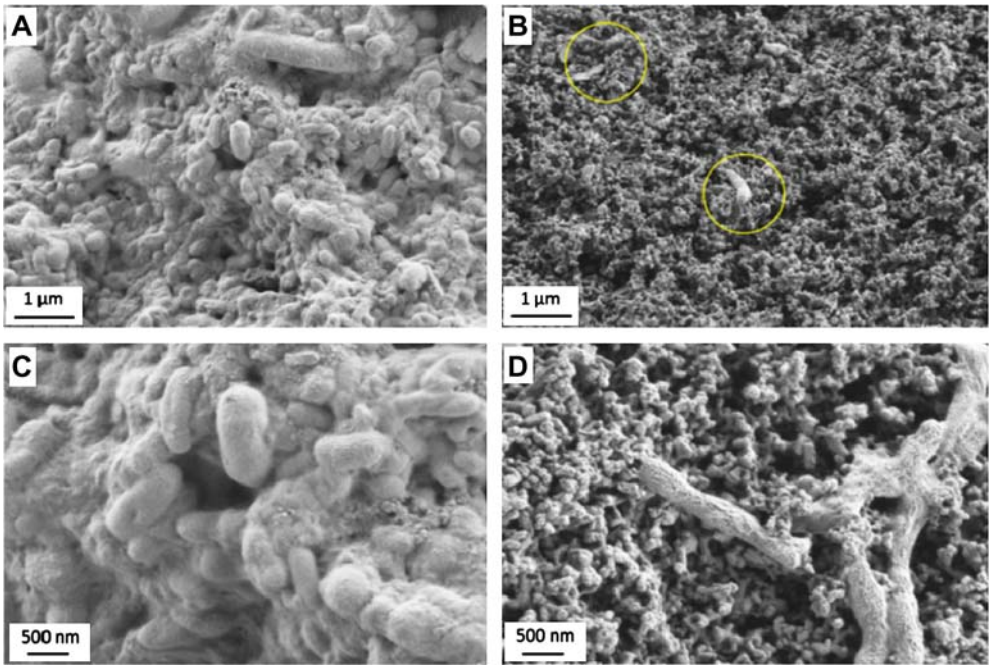

Fig. 7. Influence of PAA–ZnO np gel on biofilm development in flow-through runs in the presence of a *P. putida* S-12 suspension (10^8 CFU mL^{-1} for 72 h at Re ~ 400). HRSEM micrographs at the end of the flow-through experiments. Left panels: PAA gel without ZnO np (control) (A ×5 K, C ×10 K magnification). Right panels: composite PAA with ZnO np (B ×5 K, D ×10 K magnification). Circles denote single sporadic bacteria.

Results indicated that after 120 min of contact, no living bacteria remained. Sixty minutes of contact reduced the bacterial titer by more than 95%. These results fit with those obtained for the composite PMMA–ZnO film (see above) and are in line with literature reports [23]. The PAA–ZnO gel contained a higher concentration of ZnO np located at the surface (see Fig. 6); therefore, the bacterial reduction was improved, showing a faster and more efficient bacterial elimination.

Next, a full run in flowing conditions of the PAA–ZnO np with a high concentration of *P.putida* S-12 (10^8 CFU mL^{-1}) for 72 h was performed. HRSEM images of the surface of the gel are presented in Fig. 7. HRSEM imaging of the control PAA showed a developed biofilm layer with a 3D structure (Fig. 7 (A) and (C)). Most of the bacteria in the sample seemed intact, depicting the regular rod shape typical of *P. putida* S-12. In contrast, samples of the PAA–ZnO gel showed very few bacteria attached to the surface and no biofilm (Fig. 7(B) and (D)). Observations using a higher magnification depict a somewhat untypical bacterial rod, suggesting cell damage (Fig. 7(D)). The fact that the remaining attached bacteria did not develop into a biofilm suggested that they were dead or damaged cells. Because of the presence of ZnO, no conventional dead/live in situ staining could be performed.

3.3. Antibiofouling activity of a PMMA–ZnO np feed spacer

After proving the antibacterial feasibility of composite ZnO np films in flow regime, they were further evaluated for their antibacterial effect in filtration systems. Yang et al. [27] showed that coating a membrane or a feed spacer with nanosilver suppressed biofilm development during filtration. A feed spacer is adjacent to the membrane and is assumed to be one of the parameters influencing the initial development of biofilms [28,29]. Therefore, a cross-flow experimental cell containing a composite PMMA–ZnO np film mimicking a feed spacer and a 200-kDa polysulfone membrane was set-up in the flow-through system described above (see Fig. 1). The composite film was punctured all over (about 1-mm-diameter holes) to mimic the permeable structure of a feed spacer. Experiment runs were performed in laminar regime (Re ~ 400) with 10^8 CFU mL^{-1} of *P. putida* for 72 h. The control flow cell included a similar array with a PMMA film without ZnO np. At the end of the runs, the spacer was removed and the membranes were imaged by HRSEM (Fig. 8).

HRSEM images of the control membrane (adjacent to the PMMA film) revealed a developed biofilm in a complex 3D structure (Fig. 8(A) and (B)). Micrographs

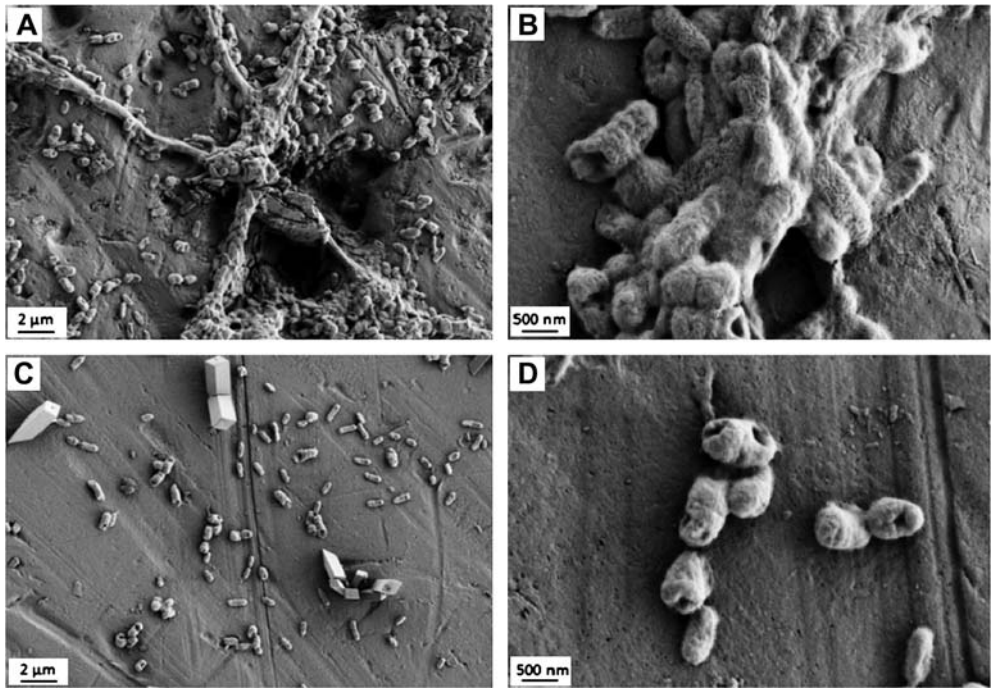

Fig. 8. HRSEM micrographs of the 200-kDa polysulfone membranes at the end of the flow-through experiment, depicting biofilm development with a 10^8 CFU mL^{-1} *P. putida* S-12 suspension in cross-flow regime (Re ~ 400) for 72 h. Upper panels: membrane adjacent to the control-PMMA spacer without ZnO np (A ×10 K, B ×50 K magnification). Bottom panels: membrane adjacent to a composite PMMA–ZnO np spacer (C ×10 K, D ×50 K magnification).

with increased magnification show that most bacteria cells are undamaged, for example intact and undistorted cells (Fig. 8(B)). Images of the membrane adjacent to the PMMA–ZnO film exhibit only single bacteria attached to the surface (Fig. 8(C) and (D)). It should be noted that the bacteria are sporadically attached on the surface in a monolayer fashion. High-magnification micrograph shows that most bacterial cells are damaged (Fig. 8(D)). Dead/live assays indicate that in the control experiment, most cells are in living state in a biofilm structure, whereas the attached bacteria in the case of composite ZnO np are in dead state (results not shown). Damage of the bacterial cell structure by ZnO is reported in the literature [25,29]. However, as far as we know, data described until now referred to static experiment conditions, while the experiments presented here were performed under flowing conditions. As flow conditions encourage biofilm development, our results reinforce the ability of the composite film to suppress biofilm development even in the case of high bacterial concentration in the feed.

4. Conclusions

The present research examined the antibacterial ability of ZnO np embedded or entrapped in polymers under flow conditions. Results indicated that although both ZnO np matrixes succeeded to repress biofilm development under flow conditions, they displayed higher antibacterial efficiency in static rather than flowing conditions. Microscopic analyses revealed that bacteria that remained attached in the presence of the ZnO np-containing films were in dead state and morphologically distorted and therefore unable to develop into biofilm. Results of ROS release from the composite film indicated that part of the antibacterial activity was lost compared to ZnO np in suspension due to the embedding in the polymer.

The antibacterial influence of the composite PAMA–ZnO np films was also evaluated in a cross-flow membrane cell system mimicking a feed spacer. Biofilm development on the adjacent polysulfone membrane was effectively suppressed.

To conclude, the novel composite polymer ZnO np displayed promising properties in biofilm prevention in flowing systems, including membrane separation, suggesting its ability to increase span time of the membranes and delay their replacement. Further research examining the time-dependent influence of a ZnO np-amended commercial feed spacer on the permeate flux and biofilm development on the membranes is underway.

Acknowledgements

This work was partially funded by the Russell Berrie Nanotechnology Institute (RBNI), Technion. The generous financial support of the Grand Water Research Institute and the Rieger foundation is gratefully acknowledged.

References

[1] H. Flemming, Reverse osmosis membrane biofouling, Exp. Thermal Fluid Sci. 14 (1997) 382–391.
[2] J.S. Baker, L.Y. Dudley, Biofouling in membrane systems—a review, Desalination 118 (1998) 81–89.
[3] K. Gopal, S.S. Tripathy, J.L. Bersillon, S.P. Dubey, Chlorination byproducts, their toxicodynamics and removal from drinking water, J. Hazard. Mater. 140 (2007) 1–6.
[4] G.A. Boorman, V. Dellarco, J.K. Dunnick, R.E. Chapin, S. Hunter, F. Hauchman, H. Gardner, M. Cox, R.C. Sills, Drinking water disinfection byproducts: Review and approach to toxicity evaluation, Rev. Environ. Health 107 (1999) 207–217.
[5] A. Asatekin, A. Menniti, S. Kang, M. Elimelech, E. Morgenroth, A.M. Mayes, Antifouling nanofiltration membranes for membrane bioreactors from self-assembling graft copolymers, J. Membrane Sci. 285 (2006) 81–89.
[6] A. Akthakul, R.F. Salinaro, A.M. Mayes, Antifouling polymer membranes with subnanometer size selectivity, Macromolecules 37 (2004) 7663–7668.
[7] Q. Li, S. Mahendra, D.Y. Lyon, L. Brunet, M.V. Liga, D. Li, P.J.J. Alvarez, Antimicrobial nanomaterials for water disinfection and microbial control: Potential applications and implications, Water Res. 42 (2008) 4591–4602.
[8] G. Applerot, A. Lipovsky, R. Dror, N. Perkas, Y. Nitzan, R. Lubart, A. Gedanken, Enhanced antibacterial activity of nanocrystalline ZnO due to increased ROS-mediated cell injury, Adv. Funct. Mater. 16 (2009) 842–852.
[9] K.M. Reddy, K. Feris, J. Bell, D.G. Wingett, C. Hanley, A. Punnoose, Selective toxicity of zinc oxide nanoparticles to prokaryotic and eukaryotic systems, Appl. Phys. Lett. 24 (2007) 2139021–2139023.
[10] J. Sawai, S. Shoji, H. Igarashi, A. Hashimoto, T. Kokugan, M. Shimizu, H. Kojima, Hydrogen peroxide as an antibacterial factor in zinc oxide powder slurry, J. Ferment. Bioeng. 86 (1998) 521–522.
[11] L.K. Adams, D.Y. Lyon, P.J.J. Alvarez, Comparative ecotoxicity of nanoscale TiO_2, SiO_2, and ZnO water suspensions, Water Res. 40 (2006) 3527–3532.
[12] J.H. Li, R.Y. Hong, M.Y. Li, H.Z. Li, Y. Zheng, J. Ding, Effects of ZnO nanoparticles on the mechanical and antibacterial properties of polyurethane coatings, Prog. Org. Coat. 64 (2009) 504–509.
[13] A.B. Moghaddam, T. Nazari, J. Badraghi, M. Kazemzad, Synthesis of ZnO nanoparticles and electrodeposition of polypyrrole/ZnO nanocomposite film, Int. J. Electrochem. Sci. 4 (2009) 247–257.
[14] Q. Peng, B. Gong, R.M. VanGundy, G.N. Parsons, "Zincone" Zinc oxide–organic hybrid polymer thin films formed by molecular layer deposition, Chem. Mater. 21 (2009) 820–830.
[15] I. Perelshtein, G. Applerot, N. Perkas, E. Wehrschetz-Sigl, A. Hasmann, G.M. Guebitz, A. Gedanken, Antibacterial properties of an in situ generated and simultaneously deposited nanocrystalline ZnO on fabrics, Appl. Mater. Interf. 1 (2009) 361–366.
[16] N. Jones, B. Ray, K.T. Ranjit, A.C. Manna, Antibacterial activity of ZnO nanoparticle suspensions on a broad spectrum of microorganisms, FEMS Microbiol. Lett. 279 (2008) 71–76.
[17] N. Padmavathy, R. Vijayaraghavan, Enhanced bioactivity of ZnO nanoparticles—an antimicrobial study, Sci. Technol. Adv. Mater. 9 (2008) 1–7.
[18] K.K. Jefferson, What drives bacteria to produce a biofilm? FEMS Microbiol. Lett. 234 (2004) 163–173.
[19] L. Eshed, S. Yaron, C.G. Dosoretz, Effect of permeate drag force on the development of a biofouling layer in a pressure-driven membrane separation system, Appl. Environ. Microbiol. 74 (2008) 7338–7347.
[20] J. Sambrook, E.F. Fritsch, T. Maniatis, Molecular Cloning: A Laboratory Manual, second ed., Cold Spring Harbor Laboratory, New York, NY, 1989.
[21] H. Ivnitsky, I. Katz, D. Minz, G. Volvovic, E. Shimoni, E. Kesselman, R. Semiat, C.G. Dosoretz, Bacterial community composition and structure of biofilms developing on nanofiltration membranes applied to wastewater treatment, Water Res. 41 (2007) 3924–3935.
[22] M.-L. Hu, Y.-K. Chen, L.-C. Chen, M. Sano, Para-aminobenzoic acid scavenges reactive oxygen species and protects DNA against UV and free radical damage, J. Nutr. Biochem. 6 (1995) 504–508.
[23] S. Chandramouleeswaran, S.T. Mhaske, A.A. Kathe, P.V. Varadarajan, V. Prasad, N. Vigneshwaran, Functional behaviour of polypropylene/ZnO–soluble starch nanocomposites, Nanotechnology 18 (2007) 385702–385710.
[24] A. Matei, I. Cernica, O. Cadar, C. Roman, V. Schiopu, Synthesis and characterization of ZnO—polymer nanocomposites, Int. J. Mater. Form. 1 (2008) 767–770.
[25] L. Zhang, Y. Jiang, Y. Ding, N. Daskalakis, L. Jeuken, M. Povey, A.J. O'Neill, D.W. York, Mechanistic investigation into antibacterial behaviour of suspensions of ZnO nanoparticles against *E. coli*, J. Nanopart. Res. 12 (2010) 1625–1636.
[26] X. Li, Y. Xing, Y. Jiang, Y. Ding, W. Li, Antimicrobial activities of ZnO powder-coated PVC film to inactivate food pathogens, Int. J. Food Sci. Technol. 44 (2009) 2161–2168.
[27] H.L. Yang, J.C. Lin, C. Huang, Application of nanosilver surface modification to RO membrane and spacer for mitigating biofouling in seawater desalination, Water Res. 43 (2009) 3777–3786.
[28] M. Modek-Gimmelshtein, R. Semiat, Investigation of flow next to membrane walls, J. Membrane Sci. 264 (2005) 137–150.
[29] J.S. Vrouwenvelder, D.A. Graf von der Schulenburg, J.C. Kruithof, M.L. Johns, M.C.M. van Loosdrecht, Biofouling of spiral-wound nanofiltration and reverse osmosis membranes: A feed spacer problem, Water Res. 43 (2009) 583–594.